

Deposition uniformity inspection in IC wafer surface

W C Li, Y T Lin, J J Jeng and C L Chang

Mechanical and Systems Research Laboratories, Industrial Technology Research
Institute, 195, Sec. 4, Chung Hsing Rd., Hsinchu, Taiwan 300, R.O.C.

E-mail: jeecool@itri.org.tw

Abstract. This paper focuses on the task of automatic visual inspection of color uniformity on the surface of integrated circuits (IC) wafers arising from the layering process. The oxide thickness uniformity within a given wafer with a desired target thickness is of great importance for modern semiconductor circuits with small oxide thickness. The non-uniform chemical vapor deposition (CVD) on a wafer surface will proceed to fail testing in Wafer Acceptance Test (WAT). Early detection of non-uniform deposition in a wafer surface can reduce material waste and improve production yields. The fastest and most low-priced inspection method is a machine vision-based inspection system. In this paper, the proposed visual inspection system is based on the color representations which were reflected from wafer surface. The regions of non-uniform deposition present different colors from the uniform background in a wafer surface. The proposed inspection technique first learns the color data via color space transformation from uniform deposition of normal wafer surfaces. The individual small region statistical comparison scheme then proceeds to the testing wafers. Experimental results show that the proposed method can effectively detect the non-uniform deposition regions on the wafer surface. The inspection time of the deposited wafers is quite compatible with the atmospheric pressure CVD time.

1. Introduction

Non-contact visual inspection based on image analysis techniques has become important for qualitative evaluation of surface quality in manufacturing. Defects that appear as local anomalies, such as stains, scratches, and wear, on material/product surfaces generally lack quantitative measures to define. They are also difficult to identify if the surrounding background contains complex patterns. Automated visual inspection has been successfully applied to a wide variety of material surfaces found in industry, such as printed circuit boards, PCBs [1-3], semiconductor wafers [4-6], liquid crystal display (LCD) panels [7-9], solar cells [10, 11], and textile fabrics [12, 13]. For PCB inspection, embedded fiducial markers on the boards allow the image under inspection to be registered with respect to the golden template for comparison. For semiconductor wafer inspection, the surface shows repetitive die patterns in the image so that the defect can be identified when it breaks the periodicity on the surface, but the uniformity inspection of a deposited wafer surface was less mentioned in technical literature. This paper focuses on the task of automatically visual inspection of color uniformity on the surface of integrated circuits (IC) wafers arising from the layering process. The non-uniform chemical vapor deposition (CVD) on a wafer surface will proceed to fail testing in Wafer Acceptance Test (WAT). Early detection of non-uniform deposition in a wafer surface can reduce material waste and improve production yields.



2. Non-uniform deposition inspection in IC wafer surface

This section presents the proposed defects detection scheme for deposited wafer images. Section 2.1 first describes the HSI color feature extraction and normal data training procedure in the IC wafer surface. Section 2.2 further discusses the defect identification scheme in the deposited wafer surface.

2.1. Color features extraction from HSI color space

HSL and HSV are the two most common cylindrical-coordinate representations of points in an RGB color model. The two representations rearrange the geometry of RGB in an attempt to be more intuitive and perceptually relevant than the Cartesian (cube) representation. A third model, common in computer vision applications, is HSI, for hue, saturation, and intensity. The hue-saturation-intensity color model has human-intuitional advantages in image processing [14] such as color image enhancement, segmentation, fusion, color-based object detection, recognition, traffic signal detection and skin detection. The HSI color space, which describes more exact color than RGB model describes for human interpretation. Though the HSI model is non-uniform in perception, it is still one of the most popular color models for image processing. In practical applications, the non-uniformity in perception can be solved by some techniques. For example, in color image segmentation the deformed boundaries can be used to enclosed the target cluster so that the perception uniformity is not so critical. The algorithm of HSI color model is as follows:

$$I = \frac{R + G + B}{3}, \quad (1a)$$

$$H = \begin{cases} \theta, & \text{if } B \leq G \\ 360^\circ - \theta, & \text{if } B > G \end{cases} \quad \text{with } \theta = \cos^{-1} \left\{ \frac{\frac{1}{2}[(R - G) + (R - B)]}{\left[(R - G)^2 + (R - B)(G - B) \right]^{\frac{1}{2}}} \right\}, \quad (1b)$$

$$S = 1 - \frac{3}{R + G + B} \min(R, G, B), \quad (1c)$$

where I and S are in the range of $[0, 1]$ and H is in the range of $[0, 360^\circ]$. Figure 1(a1) shows a normal chemical deposited wafer surface image, and (a2)-(a4) present its HSI color model images individually. Figure 1(a3) and (a4) present non-uniformity color properties from wafer surface. Figure 1(b1) shows a defect deposited wafer image and its HSI color model images individual shown in (b2)-(b4). Defect region can be found on top of wafer with triangle shape. The triangle defect region shows higher hue value than normal wafer in H color band (shown in (a4) and (b4)). Because of the non-uniformity color properties in wafer surface, the defect detection strategy can not only define an arbitrary threshold to distinguish defect region from normal background.

In this research, the normal deposited wafer images are first grabbed from camera and selected the region of interesting (ROI) to calculate statistical data as the training databases. The training databases can be constructed a group of thresholding from individual color model image. The group of thresholding is defined as the measurement of uniformity for testing wafer images. The inspected wafers also have to convert HSI color model and calculate regional statistics. The deposited wafer surface inspection scheme is described in figure 2.

2.2. Deposited wafer inspection

Figure 3 describes of training ROI and definition of parameters in wafer image. The region of interesting is given by of size $R_W \times R_H$. In this paper, we define that the patch as “cell” in the region of interesting. The cell width w_{cell} and height h_{cell} is defined by equation (2).

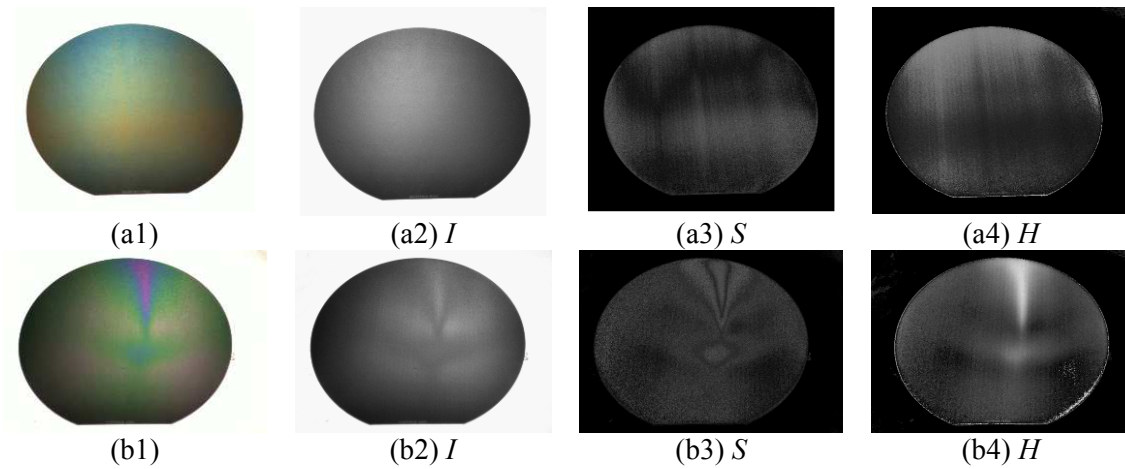


Figure 1. Deposited wafer image: (a1) normal wafer image; (a2)-(a4) the individual HSI color model images; (b1) defect wafer image; (b2)-(b4) the individual HSI color model images.

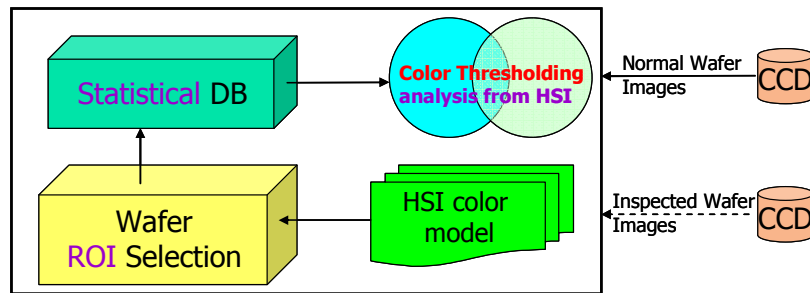


Figure 2. Deposited wafer surface inspection scheme.

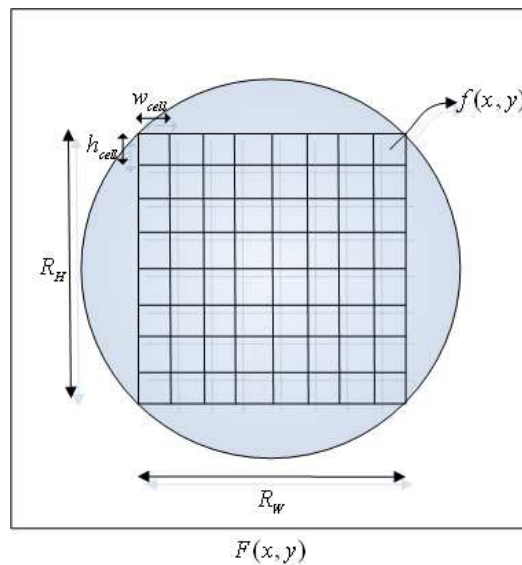


Figure 3. Description of inspection area in wafer image and size of cells.

$$w_{cell} = \frac{R_W}{N_W}, \quad h_{cell} = \frac{R_H}{N_H} \quad (2)$$

where N_W is the number of segment at R_W , and N_H is the number of segment at R_H . Therefore, the average $\mu(x, y)$ of each cell at left-top position (x, y) is calculated by

$$\mu(x, y) = \frac{1}{w_{cell} \times h_{cell}} \sum_{i=1}^{w_{cell}} \sum_{j=1}^{h_{cell}} f(x+i, y+j),$$

$$x = c \times w_{cell}, y = c \times h_{cell}, c = 0, 1, \dots, N_W \times N_H$$

and the standard deviation $\sigma(x, y)$ is calculated by

$$\sigma(x, y) = \left\{ \frac{1}{w_{cell} \times h_{cell} - 1} \sum_{i=1}^{w_{cell}} \sum_{j=1}^{h_{cell}} [f(x+i, y+j) - \mu(x, y)]^2 \right\}^{1/2}$$

Since every cell in the region of interesting is calculated its average and standard deviation, the total average $\hat{\mu}$ and total standard deviation $\hat{\sigma}$ can be given by

$$\hat{\mu} = \frac{1}{N_W \times N_H} \sum_{x=1}^{N_W \times N_H} \sum_{y=1}^{N_W \times N_H} \mu(x, y)$$

$$\hat{\sigma} = \left\{ \frac{1}{N_W \times N_H - 1} \sum_{x=1}^{N_W \times N_H} \sum_{y=1}^{N_W \times N_H} [\mu(x, y) - \hat{\mu}]^2 \right\}^{1/2} \quad (3)$$

To segment the defect cell from the background in the $F(x, y)$ image, a simple thresholding process is used. If the discriminant measure $\mu(x, y)$ of each cell is significantly larger or less than threshold, the cell $f(x, y)$ in the original image is classified as a defect one. Otherwise, it is defect-free. The simple statistic process control (SPC) is applied to set up the upper and lower limit for $\mu(x, y)$. The control limit (i.e., threshold) used to identify defect points is given by

$$U_I = \hat{\mu}_I + k \times \hat{\sigma}_I$$

$$L_I = \hat{\mu}_I - k \times \hat{\sigma}_I$$

$$U_S = \hat{\mu}_S + k \times \hat{\sigma}_S$$

$$L_S = \hat{\mu}_S - k \times \hat{\sigma}_S \quad (4)$$

where U_I and U_S is upper control limit in intensity and saturation image, and L_I and L_S is respectively lower control limit. $\hat{\mu}_I$ and $\hat{\mu}_S$ is the total average of measured value $\mu(x, y)$ for all cells in intensity and saturation image. $\hat{\sigma}_I$ and $\hat{\sigma}_S$ is the total standard deviation of cells. In this research, H color model image presents high color variation which may cause to mis-detected in normal image surface with lightly non-uniform. Therefore, we only concerned about I and S color model for wafer inspection. The parameter k is a predetermined multiplication of the standard deviation from the mean. In the experiment, the control constant k is empirically given by 2.0 for all test images. A defect cell will be set to 1 (marked with red rectangle) if the measured value is larger than U_I or U_S or less than L_I or L_S , whereas a defect-free cell will be set to 0 (do nothing) in the original image. That is,

$$f(x, y) = \begin{cases} NG(1) & \text{if } \mu(x, y) > U_I \text{ or } \mu(x, y) < L_I \\ & \text{or } \mu(x, y) > U_S \text{ or } \mu(x, y) < L_S \\ Pass(0) & \text{otherwise} \end{cases} \quad (5)$$

3. Experimental results

The proposed algorithms were implemented on an Intel Core 2, 3.4GHz CPU personal computer. The mean computation time of the proposed method was 0.5s for a 1280×1024 image (which exclude the training time). The control constant k of the statistical control limit is set at 2 for defect detection. Figure 4 shows the detection results of four normal wafer images and four defect wafer images. Figure 4(a2)-(d2) show the individual detection results of (a1)-(d1), and they are indexed with the green “PASS” symbol on the right-top of panel. They are no false alarms are generated. Figure 4(e1)-(h1) present four defect wafer images and their detection results which shown in figure 4(e2)-(h2). The individual defect cells are marked with red rectangles and indexed with red “NG” symbol to notice users.

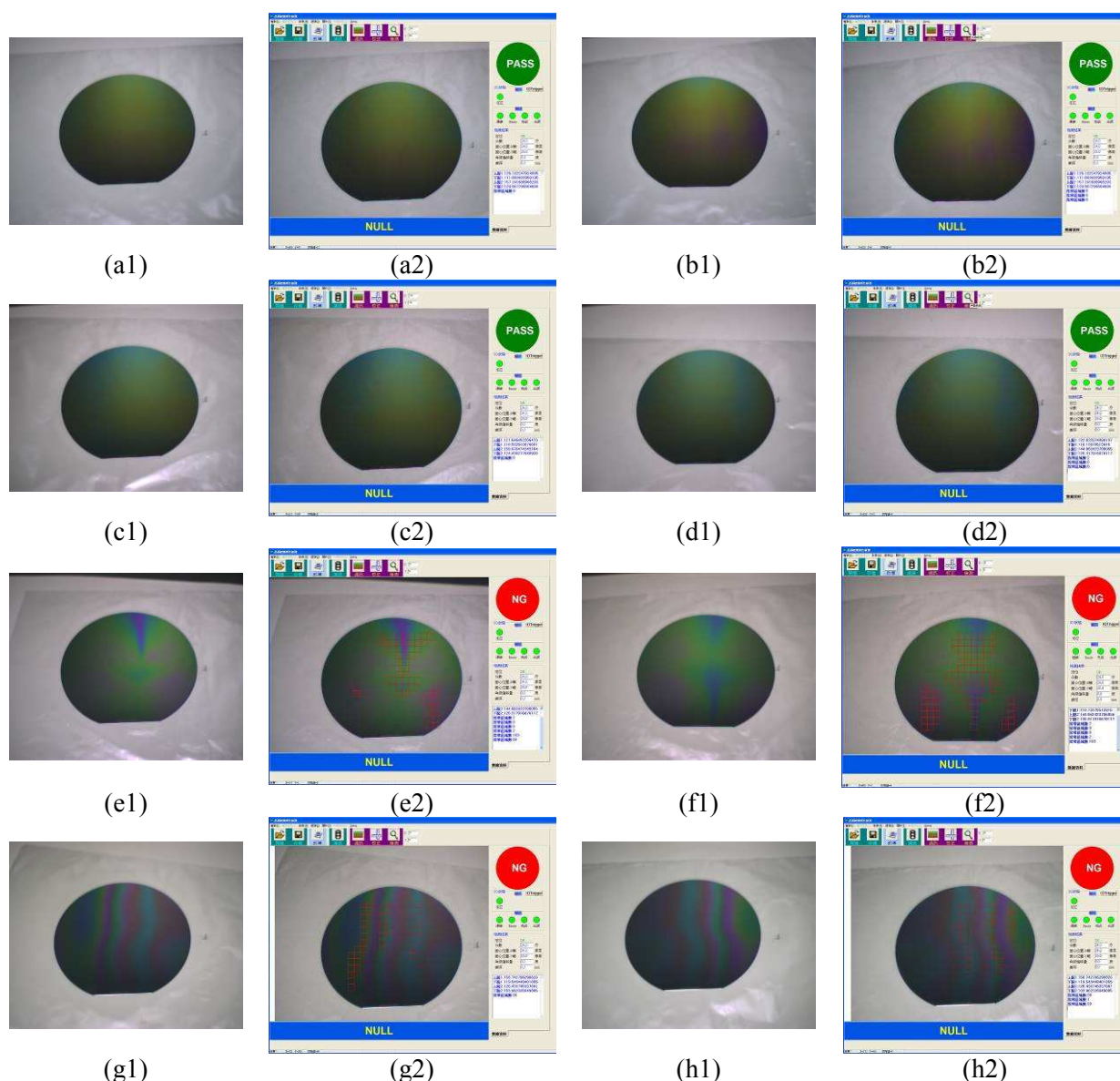


Figure 4. Detection results of deposited wafers: (a1)-(d1) four normal wafer images and individual detection results shown in (a2)-(d2); (e1)-(h1) four defect wafer images; (e2)-(h2) the individual detection results and marked defect cells with red rectangles.

4. Conclusion

This paper has proposed a defect detection scheme based on regional statistical data technique to identify non-uniform defects in deposited IC wafer images. The individual small region statistical comparison scheme then proceeds to the testing wafers. Experimental results show that the proposed method can effectively detect the non-uniform deposition regions on the wafer surface. The inspection time of the deposited wafers is quite compatible with the atmospheric pressure CVD time.

5. References

- [1] Moloney C R 1991 *IEEE Pacific Rim Conference on Communications, Computers and Signal Processing* pp. 811–814.
- [2] Yeh C H and Tsai D M 2001 “Wavelet-based approach for ball grid array (BGA) substrate conduct paths inspection,” *International Journal of Production Research*, Vol. 39, pp. 4281–4299.
- [3] Leta F R, Feliciano F F and Martins F P R 2008 “Computer vision system for printed circuit board inspection,” *ABCM Symposium Series in Mechatronics*, Vol. 3, pp. 623–632.
- [4] Su C T, Yang T and Ke C M 2002 “A neural-network approach for semiconductor wafer post-sawing inspection,” *IEEE Trans. on Semiconductor Manufacturing*, Vol. 15, pp. 260–266.
- [5] Shankara N G and Zhongb Z W 2005 “Defect detection on semi-conductor wafer surfaces,” *Microelectronic Engineering*, Vol. 77, pp. 337–346.
- [6] Yeh C H, Wu F C, Ji W L and Huang C Y 2010 A wavelet-based approach in detecting visual defects on semiconductor wafer dies”, *IEEE Trans. on Semiconductor Manufacturing*, Vol. 23, pp. 154–164.
- [7] Oh J H, Kwak D M, Lee K B, Song Y C, Choi D H and Park K H 2004 Line defect detection in TFT-LCD using directional filter bank and adaptive multilevel thresholding,” *Key Engi-neering Materials*, Vol. 270-273, pp. 233–238.
- [8] Zhang Y and Zhang J 2005 Fuzzy recognition of the defect of TFT-LCD,” *Proc. of SPIE*, pp. 233–240.
- [9] Tsai D M and Tsai H Y 2010 Low-contrast surface inspection of mura defects in liquid crystal displays using optical flow-based motion analysis,” *Machine Vision and Applications*, Vol. 22, pp. 629–649.
- [10] Seiler D 2010 “Dual exposure speeds solar cell inspection,” *Photonics Spectra*, Vol. 44, pp. 238–248.
- [11] Zhang W-J, Li D and Feng Y 2010 “Investigation of visual inspection method for silicon solar cell,” *Journal of Computer Applications*, Vol. 30, pp. 249–252.
- [12] Cho C S, Chung B M and Park M J 2005 “Development of real-time vision-based fabric inspection system,” *IEEE Transactions on Industrial Electronics*, Vol. 52, pp. 1073–1079.
- [13] Kumar A 2008 “Computer-vision-based fabric defect detection: a survey,” *IEEE Transactions on Industrial Electronics*, Vol. 55, pp. 348–363.
- [14] Chien C-L and Tseng D-C 2011 “Color image enhancement with exact HSI color model,” *International Journal of Innovative Computing, Information and Control*, Vol. 7, pp. 6691–6710.

Acknowledgments

This material is based upon work supported by the Industrial Technique Research Institute, Mechanical and Systems Research Laboratories under Grant No. C301AA4110. My thanks and appreciations also go to my colleague in developing the project and people who have willingly helped me out with their abilities.